GFZ
Helmholtz-Zentrum
POTSDAM

Originally published as:

Adjaoud, O., Steinle-Neumann, G., Jahn, S. (2011): Transport properties of Mg2SiO4 liquid at high pressure: Physical state of a magma ocean. - Earth and Planetary Science Letters, 312, 3-4, 463-470

DOI: 10.1016/j.epsl.2011.10.025

Transport properties of Mg_2SiO_4 liquid at high pressure: Physical state of a magma ocean

O. Adjaoud[a,b], G. Steinle-Neumann[a,*], S. Jahn[b]

[a] *Bayerisches Geoinstitut, Universität Bayreuth, 95440 Bayreuth, Germany*
[b] *GFZ German Research Centre for Geosciences, Section 3.3, Telegrafenberg, 14473 Potsdam, Germany*

Abstract

We use a flexible potential model to perform large-scale molecular dynamics simulations on self-diffusivity and viscosity of Mg_2SiO_4 melt up to pressures of 32 GPa and over a temperature range of 2600 to 3200 K. We find that self-diffusivity decreases and viscosity increases uniformly with pressure, the latter from values of 10^{-2} Pa s at 0 GPa to 10^{-1} Pa s at 32 GPa (2600 K). Both transport properties can be readily fit with a closed Arrhenius expression over the whole pressure and temperature range considered. Independent estimates of self-diffusivities and viscosity allow us to examine their relation through the Stokes-Einstein and the Eyring equations. While at low pressures the SiO_4 tetrahedron seems to be the viscous flow unit, bare ion diffusion becomes more dominant at high pressure. Combining previous simulation results on thermodynamic properties with the current viscosity simulations we compute a magma ocean adiabat and the associated viscosity profile. We find that viscosity in the magma ocean is $\sim 2 \cdot 10^{-2}$ Pa s near the surface, and that

*Corresponding author
Email address: g.steinle-neumann@uni-bayreuth.de (G. Steinle-Neumann)

it increases by less than 0.5 log-unit up to 35 GPa. Combining scenarios for magma ocean dimensions in the young Earth with thermodynamic properties and viscosity of Mg_2SiO_4 melt we compute a magma ocean Rayleigh number Ra in the range of 10^{28} and 10^{29}, putting the magma ocean in the dynamic regime of hard turbulence. Using scaling relations for the Nusselt number Nu at very high Ra we estimate the heat flux of the magma ocean to be in the range of 10^{18} to 10^{19} W.

Keywords: Magma Ocean, Mg_2SiO_4 Liquid, High Pressure Diffusivity, Melt Viscosity

---

October 12, 2011

1. Introduction

Viscosity of silicate melts is of central importance in many geological settings as it determines how magmas bodies cool, flow and erupt. Knowing the dependence of viscosity on temperature (T) (e.g Urbain *et al.*, 1982; Lacks *et al.*, 2007; Martin *et al.*, 2009; Nevins *et al.*, 2009), pressure P (e.g. Reid *et al.*, 2003; Liebske *et al.*, 2005; Lacks *et al.*, 2007; Martin *et al.*, 2009), composition (Urbain *et al.*, 1982; Lacks *et al.*, 2007) and water content (Lange, 1994; Hui and Zhang, 2007; Mookherjee *et al.*, 2008) is hence of great importance in geochemistry and geophysics. In the young Earth the thermal and chemical evolution of our planet was governed by physical properties of melt that made up the magma ocean (Rubie *et al.*, 2003; Solomatov, 2007). Viscosity of the silicate magma ocean is central to the understanding of convective dynamics (Abe, 1997) and its thermal evolution (Abe, 1997; Solomatov, 2007), and has a strong influence on crystal growth and settling

(Solomatov and Stevenson, 1993a,b) as well as equilibration between the core-forming metal liquid and the proto-mantle (Rubie *et al.*, 2003, 2011).

With the upper mantle and transition zone dominated by olivine, Mg_2SiO_4 liquid properties are of fundamental interest in understanding deep melts, in particular magma ocean stages of the young Earth. Despite this importance the knowledge of thermodynamic and transport properties of Mg_2SiO_4 melt from experiments is limited. This is partly caused by the high melting point of Mg_2SiO_4 (2163±25 K) (Bowen and Anderson, 1914) that has lead to extrapolations of properties from supercooled liquids to high T (e.g. Tangemann *et al.*, 2001) or extrapolation from other compositions (e.g. Lange and Carmichael, 1987; Rigden *et al.*, 1989). As the melting temperature increases rapidly with pressure (Ohtani and Kumazawa, 1981; Presnall and Walter, 1993) high P experiments on Mg_2SiO_4 melts are even more difficult and scarce. Viscosity measurements for Mg_2SiO_4 are restricted to ambient P and a limited T range (2300 K-2500 K) (Urbain *et al.*, 1982).

At high pressure, direct measurements of viscosity are based on the *falling sphere* method, in which the viscosity of a liquid can be computed from the sinking velocity of a solid sphere through a liquid by Stokes' law, monitored by X-ray radiography (Kushiro, 1978; Reid *et al.*, 2003; Liebske *et al.*, 2005). Due to the low viscosity (high velocity) the falling sphere method is extremely challenging for depolymerized melt compositions, including Mg_2SiO_4 with a nominal ratio of non-briding oxygens per tetrahedrally coordinated cation (NBO/T) of 4.

Molecular dynamics (MD) simulations provide a complementary route to explore the high P and T behavior of silicate melts, including Mg_2SiO_4 (de

Koker *et al.*, 2008; Adjaoud *et al.*, 2008; Martin *et al.*, 2009; Lacks *et al.*, 2007; Ghosh and Karki, 2011).

Ab-initio computations based on density functional theory (DFT) are accurate and transferable, but they are computationally demanding, and cell sizes for simulations of silicate liquids have been restricted up to a few hundred atoms (Stixrude and Karki, 2005; de Koker *et al.*, 2008; Sun, 2008; Sun *et al.*, 2011; Karki and Stixrude, 2010; de Koker, 2010a; Ghosh and Karki, 2011). Also, until the recent work of Ghosh and Karki (2011) run durations have been limited to a few tens of ps. This allows for accurate determination of structural and thermodynamic properties, but in order to obtain good statistics - and hence geophysically relevant precision - for the fluctuation formula that define transport properties long run durations (hundreds of ps) and large simulation cells (more than 1000 atoms) are required. Consequently, significant uncertainties are reported in self-diffusivity (de Koker *et al.*, 2008; Sun, 2008; de Koker, 2010a) and viscosity (Karki and Stixrude, 2010; Karki *et al.*, 2011) for DFT-based MD simulations.

Empirical potentials (Gale et al., 1992; Matsui, 1994; Guillot and Sator, 2007a,b; Lacks *et al.*, 2007; Martin *et al.*, 2009; Nevins *et al.*, 2009; Zhang *et al.*, 2010) are often used to efficiently explore physical properties of melts; large system sizes and long run durations, and hence transport properties, are readily accessible. However, such potentials suffer from the fact that they are typically fit to a set of experimental data and their transferability to different compositions or different thermodynamic conditions is not guaranteed.

As pointed out in the previous paragraphs these simulation approaches have limitations for a comprehensive study of transport properties at high

P and T, and here we attempt to bridge the gap between them. We apply the Aspherical Ion Model (AIM) (Aguado *et al.*, 2003; Madden *et al.*, 2006) that explicitly considers ionic polarization and shape deformation, and that is derived from electronic structure calculations. With the AIM method we have successfully studied crystalline magnesiosilicate materials over a wide range of P and T (Jahn and Madden, 2007; Jahn, 2008a; Jahn and Martonak, 2008, 2009; Jahn, 2010) and Mg_2SiO_4 liquid (Adjaoud *et al.*, 2008). Overall, the AIM results for Mg_2SiO_4 melts show good agreement with the *ab-initio* thermodynamic results (de Koker *et al.*, 2008) and experimental zero pressure viscosity (Urbain *et al.*, 1982).

Here we expand our previous work on thermodynamic and transport properties of Mg_2SiO_4 melt (Adjaoud *et al.*, 2008) and compute the P and T dependence of self-diffusivity and viscosity between 0-32 GPa and 2600-3000 K on a dense P and T grid, thightly sampling the proposed conditions for the magma ocean (e.g. Righter, 2003; Solomatov, 2007). Such a dense mesh allows us to understand and fit in detail the functional dependence of viscosity and self-diffusivity, and use the results to explore the dynamic regime of the magma ocean in the young Earth.

2. Method

The AIM model takes into account the Coulomb interaction between charged particles, short-ranged repulsion due to the overlap of the charge densities, dispersion, ionic polarization effects and ion shape deformations, and is described in detail elsewhere (Aguado *et al.*, 2003; Madden *et al.*, 2006). The set of AIM potentials used here was parameterized for the Ca-

Mg-Al-Si-O system by reference to electronic structure calculations. We use the same set of potentials that was constructed for crystalline magnesiosilicate (Jahn and Madden, 2007) and that we applied in our previous work on thermodymanic properties of Mg_2SiO_4 melt (Adjaoud *et al.*, 2008).

Molecular dynamics simulations were performed using a cubic simulation box with 2016 ions (288 formula units), similar to the simulation cell by Lacks *et al.* (2007), with a time step of 1 fs for the numerical integration of the equations of motion. Simulations are performed at constant P and T until equilibrium is achieved, then the volume (V) is held constant. T is controlled by a Nosé-Hoover thermostat (Nosé and Klein, 1983). The equilibration is performed with an isotropic barostat (Martyna *et al.*, 1994) coupled to the thermostat for 50 ps before the production run of 150 ps length is started. We explore pressures from 0 to 32 GPa, with a step of 4 GPa, and temperatures of 2600, 2800, 3000 and 3200 K. The current work extends our previous study (Adjaoud *et al.*, 2008), where we had computed the thermodynamic properties of forsterite melt in the same temperature range up to a pressure of 24 GPa, and D and η along an isotherm of 2800 K. Longer run durations allow for better statistics in computing the transport properties, including the 2800 K points. Thermodynamic parameters were found to be consistent with the previously published results, and we rely on the formulation of thermodynamic properties presented there.

Due to large system size and long trajectories we can reliably compute the self-diffusion coefficients D_α of the individual atomic species (α = O, Mg, Si) from the molecular dynamics runs via the Einstein relation (Allen and

Tildesley, 1987):

$$D_\alpha = \lim_{t \to t_{max}} \frac{1}{N_\alpha} \sum_{i=1}^{N_\alpha} \frac{\langle (\boldsymbol{r}_i(t+t_0) - \boldsymbol{r}_i(t_0))^2 \rangle}{6t}, \quad (1)$$

where $\boldsymbol{r}_i$ is the position of i^{th} ion of species α at time t, and ensemble averages (denoted by angular brackets) of the mean square displacements are taken for a specific species with a total number of ions N_α. Origin time t_0 is varied to obtain better sampling.

Shear viscosity η is computed by the Green-Kubo relation (Allen and Tildesley, 1987), integrating the autocorrelation function for the stress tensor (σ_{ij}) over time:

$$\eta = \frac{V}{k_B \cdot T} \int_0^{t_{max}} dt \langle \sigma_{ij}(t+t_0) \cdot \sigma_{ij}(t_0) \rangle. \quad (2)$$

k_B is the Boltzmann constant. Five independent shear components of the stress tensor (σ_{12}, σ_{13}, σ_{23}, $\sigma_{11} - \sigma_{22}$, $2\sigma_{33} - \sigma_{11} - \sigma_{22}$) are averaged to obtain η (Allen and Tildesley, 1987).

In contrast to simulations with smaller cells our computations do not suffer from finite size effects and both D and η are well converged. We have looked at finite cell size effects in details and find well converged results for $\sim$ 1000 atoms. Similarly, both self-diffusivity and viscosity (eqs. 1 and 2) are well converged after $\sim$ 100 ps. These constraints are beyond the current reach of *ab-initio* MD simulations.

3. Results

The self-diffusion coefficients in our simulations increase slightly with T and decrease uniformly with P (Fig. 1). At 0 GPa, the self-diffusion coefficients for O and Si are similar ($D_{\mathrm{O}} \approx D_{\mathrm{Si}}$) and smaller than for Mg. At 32

GPa, the self-diffusion coefficients for O and Mg are similar ($D_{\mathrm{O}} \approx D_{\mathrm{Mg}}$) and greater than for Si. Diffusivity results for all three species are well represented by a closed Arrhenius relation

$$D = D_0 \cdot exp\left[-\frac{E_a^D + P \cdot V_a^D}{R \cdot T}\right], \tag{3}$$

where E_a and V_a are the activation energy and volume, respectively. R is the gas constant and D_0 the pre-exponential factor (Table 1 and Fig. 1). Due to the limited P-T field of the current MD simulations the Arrhenius relations fits the simulation results well, while *ab-initio* simulations with a larger P-T range have to be fit by a modified Arrhenius relation (Ghosh and Karki, 2011).

The computed pressure dependence of D is similar to results by de Koker *et al.* (2008) and Ghosh and Karki (2011), although our D values are lower by ~ 0.3 log-units for O and Mg, and ~ 0.1 log-units for Si (Fig. 1). Classical MD simulations by Lacks *et al.* (2007) are in good agreement with the *ab-initio* simulations, while results by Martin *et al.* (2009) show considerably higher diffusivity.

We find a small activation energy for Si in the Arrhenius fit (128 kJ/mol, Table 1), consistent with the trend of activation energies to decrease with the degree of polymerization (Lesher, 2010). In addition, the activation energies for Si and O are similar (Table 1), in agreement with experimental measurements in depolymerized melts (Lesher, 2010).

Inversely proportional to self-diffusivity, viscosity η decreases with T and increases with P (Fig. 2). As for D the computed viscosities can readily be

fit with an Arrhenius fit, with η_0 as a prefactor (Table 1 and Fig. 2):

$$\eta = \eta_0 \cdot exp\left[\frac{E_a^\eta + P \cdot V_a^\eta}{R \cdot T}\right]. \quad (4)$$

At zero pressure viscosity computed here is slightly lower than the extrapolation of the experimental measurements of Urbain *et al.* (1982) to 2800 K based on a Vogel-Fulcher-Tammann fit (Fig. 2). Simulations at lower temperatures can not be compared to experimental measurements directly: As the melting temperature is approached locally heterogeneous structure leads to altered dynamics of the melt with non-Arrhenian behavior (Angell *et al.*, 2000) that can not readily be captured by MD simulations due to size and time restrictions. A similar deviation between *ab-initio* MD results and measurements has recently been described and discussed by Karki *et al.* (2011) for $CaAl_2Si_2O_8$ anorthite liquid.

Viscosities computed here are slightly larger than results from the *ab-initio* computations (~ 0.2 log-units) (Ghosh and Karki, 2011) and those from the classical MD, which fall below our results by ~ 0.3 log-units (Lacks *et al.*, 2007) and ~ 0.5 log-units (Martin *et al.*, 2009), respectively. This discrepancy is consistent with their larger values of diffusion constants. Viscosities from these studies follow a similar pressure trend as ours.

In comparison to viscosity estimates on $MgSiO_3$ we find our results to be within error bounds of the *ab-initio* simulations by Karki and Stixrude (2010) for much of the pressure range covered (Fig. 2), confirming the similarity between thermodynamic and transport properties of Mg_2SiO_4 and $MgSiO_3$ melts. For $MgSiO_3$ the results from classical MD by Lacks *et al.* (2007) and Nevins *et al.* (2009) yield values on η that are similar to the *ab-initio* simulations.

As for D the limited P-T range of simulations allows us to represent η with a classical Arrhenius fit (eq. 4), while the *ab-initio* simulations over a wide P-T range require a modified Arrhenius equation for Mg_2SiO_4 (Ghosh and Karki, 2011) or a modified Vogel-Fulcher-Tammann equation for $MgSiO_3$ (Karki and Stixrude, 2010).

4. Discussion

Measurements on O self-diffusivity for $CaMgSi_2O_6$ diopside (NBO/T=2) show an initial decrease of D with P, with a minimum in the range of 9-10 GPa and a subsequent increase up to the P limit of the experiment (Reid *et al.*, 2001, 2003), contrary to the behavior of polymerized melts for which an initial increase in D with P is followed by a decrease, e.g. for $NaAlSi_3O_8$ albite (NBO/T=0) and $Na_3AlSi_7O_{17}$ sodium aluminosilicates (NBO/T=0.25) (Poe and Rubie, 2000). *Ab-initio* molecular dynamics simulations on diopside (Sun, 2008; Sun *et al.*, 2011) have attributed the local minimum in oxygen self-diffusivity to the presence of five-fold coordinated Mg and the maximum by the dominance of five-fold coordinated Si. Both of these environments can be understood as transitional states in which bonds break and form readily (Lesher, 2010). A similar behavior has been predicted for the viscosity of $MgSiO_3$ enstatite liquid (NBO/T=2), with a minimum in η near 5 GPa at 3000 K (Karki and Stixrude, 2010).

Despite five-fold coordinated Si playing a major role in the structure of liquid Mg_2SiO_4 based on *ab-initio* molecular dynamics simulations (de Koker *et al.*, 2008), no maximum in D was predicted in their study, in Ghosh and Karki (2011), here, or in MD simulations using other classical potentials

(Lacks *et al.*, 2007; Martin *et al.*, 2009).

Transport properties D and η of silicate melts have often been related via the Eyring equation (Eyring, 1936):

$$D = \frac{k_B \cdot T}{\lambda \cdot \eta}, \tag{5}$$

where k_B is the Boltzmann constant and λ is a parameter with the dimension of length. Using the viscosity and self-diffusion coefficients of O, Si and Mg at 0 GPa, we compute λ to be equal 25 Å, 30 Å and 9 Å, respectively (Fig. 3). With pressure, λ remains almost constant for Mg (increasing to 11 Å at 32 GPa) and decreases for O and Si, reaching values of 11 Å and 19 Å at 32 GPa, respectively. This is broadly consistent with the recent *ab-inito* simulations by Ghosh and Karki (2011) that also show a decrease in λ for Si and O, and an almost constant value for Mg. However, the absolute values of λ at low pressure for O and Si in our study are somewhat larger than those by Ghosh and Karki (2011), and λ for O decreases faster in their study (Fig. 3).

The nature and value of the proportionality factor λ has been the subject of much debate in the experimental and computational literature. Traditionally, λ has been interpreted as the jump distance of the diffusing species that acts as the viscous flow unit (usually assumed to be O^{2-}). From experiments it was found that $\lambda = 2R_O$, with $R_O = 1.4$ Å the ionic radius of oxygen (Shannon and Prewitt, 1969), yields good correlation between oxygen self-diffusivity and η in polymerized melts (Shimizu and Kushiro, 1984; Poe *et al.*, 1997), while more depolymerized melts require a larger λ. For diopside (NBO/T=2) Reid *et al.* (2003) reported λ=4.5 Å and Dunn (1982) estimated an even larger value of $\sim$ 18 Å for 40% diopside - 60% anorthite

melt (NBO/T=0.98). For Mg_2SiO_4 melt (NBO/T=4), experimental data are not available, but the MD simulations suggest a similar or even larger value of λ: 17 Å from Ghosh and Karki (2011), 18 Å from Martin *et al.* (2009), 22 Å from (Lacks *et al.*, 2007) and 25 Å from our study. Clearly, such large values of λ do not correspond to any realistic jump distance in the melt.

In the original work by Eyring (1936), the proportionality constant of equation 5 is not a single jump distance, λ, but rather a combination $(\lambda_2\lambda_3/\lambda_1)$ of three distances λ_1, λ_2 and λ_3, which are the distance of two neighboring layers of molecules sliding past each other, the intermolecular distance in the direction of motion, and an intermolecular distance perpendicular to λ_1 and λ_2, respectively. The effective volume of the diffusing species can then be assumed to correspond to $\lambda_1\lambda_2\lambda_3 = V/N$, where V is the volume of the simulation cell and N is the number of those particles that determine viscous flow.

Here we consider O^{2-} or SiO_4^{4-} as diffusing species. Using the values of λ from Fig. 3, the calculated values for λ_1 and $(\lambda_2\lambda_3)^{1/2}$ are given in Table 2. At 0 GPa, the value of λ_1 (0.94 Å) determined for the self-diffusion of O^{2-} species is considerably smaller than the ionic radius of O^{2-} (1.4 Å). The value of λ_1 (1.72 Å) determined for SiO_4^{4-} seems more realistic, as it is similar to the average Si-O bond length (1.62 Å). This is still somewhat smaller than the radius of an SiO_4^{4-} unit, which is approximated by subtracting the radius of the Mg^{2+} ion from the first neighbor Si-Mg distance (2.16 Å). Also, the corresponding value $(\lambda_2\lambda_3)^{1/2}$ of 7.35 Å appears to be a rather large jump distance in the melt, although it is much smaller than $\lambda = 25$ Å discussed above.

An alternative to the Eyring equation, which was derived for diffusion of particles of the same size, is the Stokes-Einstein relation

$$D = \frac{k_B \cdot T}{\xi \cdot \pi \cdot R_d \cdot \eta}, \tag{6}$$

which describes the motion of large particles in a solvent. In this case, R_d is the hydrodynamic radius of the diffusing species and ξ is a constant ranging between 4 and 6 depending on the boundary conditions. Assuming SiO_4^{4-} as spheres with a radius of 2.16 Å moving in a solvent of Mg^{2+} cations and applying free slip boundary conditions ($\xi = 4$), the Stokes-Einstein relation yields results that correspond to the Si self-diffusion coefficient within error bars (see Fig. 3).

The latter is representative for the diffusion of SiO_4^{4-} units. These results suggest that at low pressure the diffusing species determining the viscous behavior of the melt are SiO_4^{4-} tetrahedra and that the Stokes-Einstein relation is more appropriate than the Eyring equation for Mg_2SiO_4 melt.

At high pressure, SiO_4^{4-} tetrahedra become dynamically less stable and Si coordinations higher than four are predicted for Mg_2SiO_4 (Adjaoud *et al.*, 2008; de Koker *et al.*, 2008). Frequent formation and breaking of oxygen-cation bonds appear to change the nature of the diffusing species that control viscosity. At 32 GPa and assuming O^{2-} as the diffusing species, λ_1 of the Eyring model is similar to the ionic radius of O^{2-} and $(\lambda_2\lambda_3)^{1/2}$ yields a realistic jump distance of $\sim 2.5\ R_{\mathrm{O}}$ (see Table 2). Reasonable distances are also obtained assuming diffusing SiO_4^{4-} units (Table 2), but $(\lambda_2\lambda_3)^{1/2}$ of 5.64 Å is still relatively large as a jump distance. Such a transition in diffusion characteristics is also consistent with the results from the *ab-initio* simulations (Ghosh and Karki, 2011), although there the transition would

be predcited at lower pressures, consistent with the decrease in λ for oxygen (Fig. 3)

Interestingly, the Stokes-Einstein relation provides correct diffusion coefficients over the whole pressure range if Mg^{2+} with a radius of 0.86 Å is considered as the diffusing species (Fig. 3). Further systematic studies on different melts over a wide temperature range are needed to assess the relevance of this observation, but this is beyond the scope of this paper.

5. Implication for Magma Ocean Structure

Energy released by impacts during accretion of the Earth (Chambers and Wetherill, 1998) and radiogenic heating of short lived isotopes like ^{26}Al (Walter and Tronnes, 2004) in its early history has almost invariably resulted in melting of large parts of the Earth, leading to a magma ocean of uniform depth (Tonks and Melosh, 1993). The depth of the magma ocean is subject of current debate, but if differentiation of the core is assumed to have happened essentially in one stage, equilibration of elements between the dense iron melt ponding at the base of the silicate liquid can be used as a geochemical signature of equilibration pressure at the magma ocean solidus and hence magma ocean depth (Wood *et al.*, 2006; Corgne *et al.*, 2009). Using high pressure partition coefficients for siderophile elements, its depth has been established in the range of 25-45 GPa (Wood *et al.*, 2006; Corgne *et al.*, 2009), although other elements suggest that a uniform equilibration pressure between metal and silicate melt is unlikely (Mann *et al.*, 2009; Rubie *et al.*, 2011), and scenarios have been considered with the whole mantle molten (e.g. Lee *et al.*, 2010).

With a magma ocean depth of $\sim$ 25-40 GPa, and thermodynamic and transport properties of Mg_2SiO_4 and $MgSiO_3$ liquids being very similar (Lacks *et al.*, 2007; Adjaoud *et al.*, 2008; de Koker and Stixrude, 2009; Karki *et al.*, 2009; Stixrude *et al.*, 2009; Karki and Stixrude, 2010; Ghosh and Karki, 2011), it is possible to explore the structure of the magma ocean by considering the thermodynamic and viscosity results of Mg_2SiO_4 melt computed here.

In a rapidly convecting magma ocean the Grüneisen parameter γ governs the thermal structure of the magma ocean $(\partial T/\partial P)_S$ through

$$\left(\frac{\partial T}{\partial P}\right)_S = \frac{\gamma \cdot T}{K_S}, \tag{7}$$

with K_S the adiabatic bulk modulus. The isothermal bulk modulus $K_T = \rho \cdot (\partial P/\partial \rho)$ must be converted to $K_S = K_T \cdot (1 + \alpha \cdot \gamma \cdot T)$, where α is the thermal expansion coefficient and ρ the density of the liquid. Both α and ρ as a function of P and T are computed self-consistently from the previously published thermodynamic results for Mg_2SiO_4 (Adjaoud *et al.*, 2008).

We have calculated adiabats with potential temperatures of $T_0 = 2163$ K, the melting point of forsterite (Bowen and Anderson, 1914), and $T_0 = 2500$ K as an envelope for the thermal profile in the magma ocean (Fig. 4). The colder adiabat would intersect the mantle liquidus at $P \sim 25$ GPa and the solidus at $P \sim 30$ GPa, consistent with adiabats by Stixrude *et al.* (2009) and de Koker and Stixrude (2009) (Fig. 4). This would not lead to a magma ocean depth in agreement with the geochemical evidence (Wood *et al.*, 2006; Corgne *et al.*, 2009). The hotter adiabat ($T_0 = 2500$ K) remains superliquidus to pressures of $\sim$ 35 GPa and the solidus would be reached at $\sim$ 45 GPa, leading to a deep magma ocean. With $T = 3200$ K at 35

GPa this adiabat is lower by ∼150-300 K compared to recent assessments of MD simulations (Stixrude *et al.*, 2009; de Koker and Stixrude, 2009). The extrapolated intersection with the solidus at ∼ 45 GPa and 3400 K, however, is in agreement with the temperature (3000-3500 K) established from equilibration of liquid metal and silicate at comparable P (Corgne *et al.*, 2009). The adiabatic gradient computed here (Fig. 4) is considerably lower than the komatiite adiabat based on shock-wave experiments used previously for the Hadean magma ocean temperature profile (Miller *et al.*, 1991), due to a smaller γ_0.

Using the adiabat with $T_0 = 2500$ K we can establish a viscosity profile of the magma ocean using the viscosity fit (Table 1) and find $\eta = 2 \cdot 10^{-2}$ Pa s at the surface, and viscosity to vary only weakly with pressure (Fig. 4). Viscosity along the adiabat changes by less than 0.5 log-units up to 35 GPa. Viscosity along the colder adiabat is higher by ∼0.1 log-unit at the surface and by ∼0.3 log-units at 35 GPa. The viscosity profile obtained here is in good agreement with those recently computed for $MgSiO_3$ (Karki and Stixrude, 2010) and Mg_2SiO_4 (Ghosh and Karki, 2011) (Fig. 4). Based on these studies, viscosity does not exceed 0.1 Pa s even for the whole mantle molten.

A viscosity minimum (2-3 GPa) and maximum (8 GPa) in the magma ocean as implicated previously based on peridotite measurements (Liebske *et al.*, 2005) combined with an initially colder but steeper adiabat (Miller *et al.*, 1991) is unlikely along the temperature profile of the magma ocean determined here: The minimum in η at 3000 K and 5 GPa for enstatite melt computed by *ab-inito* simulations (Karki and Stixrude, 2010) is not reflected

in the viscosity profile (Fig. 4).

In a magma ocean of 30-45 GPa depth viscosity can be assumed constant for all practical purposes with a value of $\eta = 4 \cdot 10^{-2}$ Pa s. After crystallization starts in the magma ocean, effective viscosity (η_e) is rescaled by the fraction (Φ) of the crystals formed, following a scaling law developed by Roscoe (1952):

$$\eta_e = \frac{\eta}{(1 - \Phi/\Phi_m)^{5/2}}. \tag{8}$$

The critical packing fraction of crystals (Φ_m) is determined experimentally to be $\sim$0.6 (Lejeune and Richet, 1995). Even up to 25% crystallization viscosity will change by less than a factor of 5.

The vigor of convection in the Hadean magma ocean is governed by its Rayleigh number:

$$Ra = \frac{\alpha \cdot c_P \cdot \rho^2 \cdot g \cdot \Delta T \cdot L^3}{k \cdot \eta}. \tag{9}$$

Using planetary physical parameters (gravitational acceleration g and depth of the magma ocean L), thermodynamic properties of Mg_2SiO_4 melt along the adiabat (thermal expansivity α, heat capacity c_P, and mean density ρ) and the viscosity value just established, we compute Ra for two scenarios (Table 3): (1) a magma ocean with a depth of 30 GPa ($\sim$ 750 km) in the accretion stage, i.e. with reduced radius of the planet (r) and consequently g, and (2) a magma ocean with depth of the current mantle. Thermal conductivity k of silicate melts at high pressures is unexplored, but ambient pressure measurements on lavas (Buttner *et al.*, 2000), synthetic samples (Kang and Morita, 2006), and molecular dynamics estimates of solid minerals at P and T of the deep mantle (de Koker, 2010b) provide useful bounds (Table 3).

With a dense insulating atmosphere (Hashimoto *et al.*, 2007; Abe and Matsui, 1986) the temperature difference ΔT throughout the magma ocean is that of the adiabat.

In the two scenarios $Ra \sim 10^{28}$ and $Ra \sim 10^{29}$, respectively (Table 3). This is consistent with values used in the literature (Rubie *et al.*, 2003; Höink *et al.*, 2006; Solomatov, 2007), putting the magma ocean in the dynamic regime of hard turbulence (Solomatov, 2007; Yuen *et al.*, 1993).

The total convective heat flow can be computed from scaling laws, using the definition of the Nusselt number Nu:

$$Nu = \frac{h \cdot L}{k}, \tag{10}$$

which measures convective over conductive heat transfer. The convective heat transfer coefficient h is defined as:

$$h = \frac{q}{A \cdot \Delta T}. \tag{11}$$

A is the surface area over which heat is lost - in the case of a planet the surface of the spherical body - and equations 10 and 11 can be solved for the total heat flux q:

$$q = \frac{k \cdot A \cdot \Delta T}{L} \cdot Nu. \tag{12}$$

Scaling laws can be used relating Ra, Nu and the Prandtl number Pr. Pr measures the ratio of momentum to thermal diffusion

$$Pr = \frac{\eta \cdot c_P}{k}. \tag{13}$$

For high Ra Shraiman and Siggia (1990) have established such a scaling relation, with a correction factor for the aspect ratio of the *flow container* ($\Gamma = 2\pi \cdot r/L$ for the high aspect ratio of a magma ocean):

$$Nu \approx 0.27 \cdot Pr^{-1/7} \cdot Ra^{2/7} \cdot \Gamma^{-3/7}. \quad (14)$$

Substituing this relation into equation 12 the total heat flux can be computed according to:

$$q = 1.08 \cdot \pi \cdot k \cdot \Delta T \frac{r^2}{L} \cdot Ra^{2/7} \cdot Pr^{-1/7} \cdot \Gamma^{-3/7}. \quad (15)$$

For the two magma ocean scenarios considered (Table 3) we find a heat flow of 10^{18} and 10^{19} W, respectively.

The Prandtl number we obtain ($Pr \sim 10$ and $Pr \sim 5$, respectively) for both scenarios (Table 3) are consistent with some magma ocean work (Höink *et al.*, 2006), and at the lower limit of other estimates (Solomatov, 2007). Due to high Ra, rotation - and hence the Coriolis force - does not contribute to convective flow and heat flux (Canuto and Dubovikov, 1998; Solomatov, 2007).

6. Conclusions

Simulations on transport properties of Mg_2SiO_4 by molecular dynamics at high pressures (0-32 GPa) and temperatures (2600-3200 K) using an advanced ionic interaction model yield results on self-diffusivity and viscosity that can readily be fit with an Arrhenius equation. Our results suggest that diffusion mechanisms controlling the viscous flow in Mg_2SiO_4 melt are different between ambient and high pressures. For fully depolymerized melts at

ambient pressure, the traditional use of the Eyring equation to describe the relation between the two transport properties does not seem to be appropriate. Further systematic studies on a range of silicate melt compositions are needed to identify the interplay between diffusing species and viscous flow units.

Combining a thermodynamic model for Mg_2SiO_4 melt (Adjaoud *et al.*, 2008) with the viscosity fit we are able to constrain an adiabat and a related viscosity profile through the magma ocean: viscosity of the magma ocean is $\sim 2 \cdot 10^{-2}$ Pa s near the surface and varies by < 0.5 log-unit along the adiabat up to 35 GPa, in general agreement with *ab-initio* simulations on the viscosity of $MgSiO_3$ (Karki and Stixrude, 2010) and Mg_2SiO_4 (Ghosh and Karki, 2011) melts. The thermodynamic data and constraints on viscosity allow us to qualitatively consider the dynamic regime of the magma ocean for two scenarios (magma oceans with a depth of 750 km and 2740 km) by establishing values of dimensionless fluid dynamics parameters for the Rayleigh ($10^{28} \leq Ra \leq 10^{29}$) and Prandlt number ($5 \leq Pr \leq 10$). These values for Ra and Pr are consistent with previous etimates for the magma ocean (Höink *et al.*, 2006; Solomatov, 2007), and put the magma ocean in the regime of hard turbulence. Through Nusselt number (Nu) scaling laws for very high Ra we are able to estimate the total heat flux of the Earth in the magma ocean stage to be in the range of 10^{18}-10^{19} W. Further tighting of these constraints will depend on future work in geochemistry and simulations of accretion and differentiation of the Earth in order to determine the depth of the magma ocean and size of the Earth at the magma ocean stage.

7. Acknowledgments

This work was funded by the State of Bavaria through the Graduate School "Oxides" in the Elitenetzwerk Bayern with a fellowship to OA and the German Research Foundation with grants to GSN (STE1105/5-1) and SJ (JA1469/4-1) . Computations were in part performed at the Leibniz Computer Center Munich. We greatly appreciate helpful discussion with N. de Koker, D. Dobson, D. Frost, M. Evonuk, and D.C. Rubie. Comments by Ch. Liebske and an anonymous reviewer significantly improved the manuscript.

References

Abe, Y., 1997. Thermal and chemical evolution of the terrestrial magma ocean. Phys. Earth Planet. Inter. **100**, 27-39.

Abe, Y., Matsui, T., 1986. Early evolution of the Earth: accretion, atmosphere formation, and thermal history. J. Geophys. Res. **91**, 291-302.

Adjaoud, O., Steinle-Neumann, G., Jahn, S., 2008. Mg_2SiO_4 liquid under high pressure from molecular dynamics. Chem. Geol. **256**, 184-191.

Aguado, A., Bernasconi, L., Jahn, S., Madden, P.A., 2003. Multipoles and interaction potentials in ionic materials from planewave-DFT calculations. Faraday Discuss. **124**, 171-184.

Allen, M.P., Tildesley, D.J., 1987. Computer Simulation of Liquids. Oxford University Press, New York.

Angell, C.A., Ngai, K.L., McKenna, G.B., McMillan, P.F., Martin, S.J 2000. Relaxation in glassforming liquids and amorphous solids. J. Appl Phys. **88**, 3113-3157.

Bowen, N.L., Andersen, O., 1914. The binary system MgO-SiO_2. Am. J. Sci. **37**, 487-500.

Buttner, R., Zimanowski, B., Lenk, C., Koopmann, A., Lorenz, V., 2000. Determination of thermal conductivity of natural silicate melts. Appl. Phys. Lett. **77**, 1810-1812.

Canuto, V.M., Dubovikov, M.S., 1998. Two Scaling Regimes for Rotating Rayleigh-Bénard Convection. Phys. Rev. Lett. **80**, 281-284.

462 Chambers, J.E., Wetherill, G.W., 1998. Making the Terrestrial Planets: N-
463 Body Integrations of Planetary Embryos in Three Dimensions. Icarus **136**,
464 304-327.

465 Corgne, A., Siebert, J., Badro, J., 2009. Oxygen as a light element: A solution
466 to single-stage core formation. Earth Planet. Sci. Lett. **288**, 108-114.

467 de Koker, N.P., Stixrude, L., Karki, B.B., 2008. Thermodynamics, struc-
468 ture, dynamics, and freezing of Mg_2SiO_4 liquid at high pressure. Geochim.
469 Cosmochim. Acta **72**, 1427-1441.

470 de Koker, N.P., Stixrude, L., 2009. Self-Consistent Thermodynamic Descrip-
471 tion of Silicate Liquids, with Application to Shock Melting of MgO Peri-
472 clase and $MgSiO_3$ Perovskite. Geophys. J. Int. **178**, 162-179.

473 de Koker, N.P., 2010. Structure, Thermodynamics, and Diffusion in
474 $CaAl_2Si_2O_8$ Liquid from First-Principles Molecular Dynamics. Geochim.
475 Cosmochim. Acta **74**, 5657-5671.

476 de Koker, N.P., 2010. Thermal Conductivity of MgO Periclase at High Pres-
477 sure: Implications for the D" Region. Earth Planet. Sci. Lett. **292**, 392-398.

478 Dunn, T., 1982. Oxygen diffusion in three silicate melts along the join
479 diopside-anorthite. Geochim. Cosmochim. Acta **46**, 2293-2299.

480 Eyring, H., 1936. Viscosity, Plasticity, and Diffusion as Examples of Absolute
481 Reaction Rates. J. Chem. Phys. **4**, 283-291.

482 Gale, J.D., Catlow, C.R.A., Mackrodt, W.C., 1992. Periodic *ab initio* deter-

mination of interatomic potentials for alumina. Modell. Simul. Mater. Sci. Eng. **1**, 73-81.

Ghosh, D. B., Karki, B. B., 2011. Diffusion and viscosity of Mg_2SiO_4 liquid at high pressure from first-principles simulations. Geochim. Cosmochim. Acta **75**, 4591-4600.

Guillot, B., Sator, N., 2007. A computer simulation study of natural silicate melts. Part I: Low pressure properties. Geochim. Cosmochim. Acta **71**, 1249-1265.

Guillot, B., Sator, N., 2007. A computer simulation study of natural silicate melts. Part II: High pressure properties. Geochim. Cosmochim. Acta **71**, 4538-4556.

Hashimoto, G.L., Abe, Y., Sugita, S., 2007. The chemical composition of the early terrestrial atmosphere: Formation of a reducing atmosphere from CI-like material. J. Geophys. Res. **112**, E05010.

Höink, T., Schmalzl, J., Hansen, U., 2006. Dynamics of metal-silicate separation in a terrestrial magma ocean. Geochem. Geophys. Geosyst. **7**, Q09008.

Hui, H., Zhang, Y., 2007. Toward a general viscosity equation for natural anhydrous and hydrous silicate melts. Geochim. Cosmochim. Acta **71**, 403-416.

Ito, E., Kubo, A., Katsura, T., Walter, M.J., 2004. Melting experiments of mantle materials under lower mantle conditions with implications for magma ocean differentiation. Phys. Earth Planet. Inter. **143**, 397-406.

505 Jahn, S., Madden P.A., 2007. Modeling Earth materials from crustal to
506 lower mantle conditions: A transferable set of interaction potentials for
507 the CMAS system. Phys. Earth Planet. Inter. **162**, 129-139.

508 Jahn, S., Martoňák, R., 2008. Plastic deformation of orthoenstatite and the
509 ortho- to high-pressure clinoenstatite transition: A metadynamics simula-
510 tion study. Phys. Chem. Minerals **35**, 17-23.

511 Jahn, S., 2008. High-pressure phase transitions in $MgSiO_3$ orthoenstatite
512 studied by atomistic computer simulation. Am. Mineral. **93**, 528-532.

513 Jahn, S., Martoňák, R., 2009. Phase behavior of protoenstatite at high pres-
514 sure studied by atomistic simulations. Am. Mineral. **94**,950-956.

515 Jahn, S., 2010. Integral modeling approach to study the phase behavior of
516 complex solids: application to phase transitions in $MgSiO_3$ pyroxenes. Acta
517 Cryst. A **66**, 535-541.

518 Kang, Y., Morita, K., 2006. Thermal conductivity of the CaO-Al_2O_3-SiO_2
519 system. ISIJ INTERNATIONAL **46**, 420-426.

520 Karki, B.B., Bhattarai, D., Mookherjee, M., Stixrude, L., 2009.
521 Visualization-based analysis of structural and dynamical properties of sim-
522 ulated hydrous silicate melt. Phys. Chem. Miner. **37**, 103-117.

523 Karki, B.B., Bohara, B., Stixrude, L., 2011. First-principles study of diffu-
524 sion and viscosity of anorthite ($CaAl_2Si_2O_8$) liquid at high pressure. Am.
525 Mineral. **96**, 744-751.

526 Karki, B.B., Stixrude, L., 2010. Viscosity of $MgSiO_3$ liquid at mantle condi-
527 tions: implications for early magma ocean. Science **328**, 740-742.

528 Kushiro, I., 1978. Density and viscosity of hydrous calc-alkaline andesite
529 magma at high pressure. Annu. Rep. 1977-78: Geophys. Lab., Carnegie
530 Inst, Washington, 675-677.

531 Lacks, D.L., Rear, D.B., Van Orman, J.A., 2007. Molecular dynamics in-
532 vestigation of viscosity, chemical diffusivities and partial molar volumes of
533 liquids along the MgO-SiO_2 join as functions of pressure. Geochim. Cos-
534 mochim. Acta **71**, 1312-1323.

535 Lange, R.A., 1994. The effect of H_2O, CO_2 and F on the density and viscosity
536 of silicate melts. Rev. Mineral. **30**, 331-369.

537 Lange, R.A., Carmichael, I.S.E., 1987. Densities of Na_2O-K_2O-CaO-MgO-
538 FeO-Fe_2O_3-Al_2O_3-TiO_2-SiO_2 liquids: new measurements and derived par-
539 tial molar properties. Geochim. Cosmochim. Acta **51**, 2931-2946.

540 Lee, C.T.A., Luffi, P., Höink T., Li J., Dasgupta, R., Hernlund, J. 2010.
541 Upside-down differentiation and generation of a 'primordial' lower mantle.
542 Nature **463**, 930-933.

543 Lejeune, A.M., and Richet, P., 1995. Rheology of crystal-bearing silicate
544 melts: an experimental study at high viscosities. J. Geophys. Res. **100**,
545 4215-4229.

546 Lesher, C.E., 2010. Self-diffusion in Silicate Melts: Theory, Observations and
547 Applications to Magmatic Systems. Rev. Mineral. Geochem. **72**, 269-309.

548 Liebske, C., Schmickler, B., Terasaki, H., Poe, B.T., Suzuki, A., Funakoshi,
549 K., Ando, R., Rubie, D.C., 2005. Viscosity of peridotite liquid up to 13
550 GPa: Implications for magma ocean viscosities. Earth Planet. Sci. Lett.
551 **240**, 589-604.

552 Madden, P.A., Heaton, R., Aguado, A., Jahn, S., 2006. From first-principles
553 to material properties. J. Mol. Struct. (Theochem) **771**, 9-18.

554 Mann, U., Frost, D.J., Rubie, D.C., 2009. Evidence for high-pressure core-
555 mantle differentiation from the metalsilicate partitioning of lithophile and
556 weakly-siderophile elements. Geochim. Cosmochim. Acta **73**, 7360-7386.

557 Martin, G.B., Spera, F.J., Ghiorso, M.S., Nevins, D., 2009. Structure, ther-
558 modynamics, and transport properties of molten Mg_2SiO_4: Molecular dy-
559 namics simulations and model EOS. Am. Mineral. **94**, 693-703.

560 Martyna, G.J., Tobias, D.J., Klein, M.L., 1994. Constant pressure molecular
561 dynamics algorithms. J. Chem. Phys. **101**, 4177-4189.

562 Matsui, M., 1994. A transferable interatomic potential model for crystals and
563 melts in the system CaO-MgO-Al_2O_3-SiO_2. Miner. Mag. **58A**, 571-572.

564 Miller, G.H., Stolper, E.M., Ahrens, T.J., 1991. The Equation of State of
565 a Molten Komatiite 2. Application to Komatiite Petrogenesis and the
566 Hadean Mantle. J. Geophys. Res. **96**, 11849-11864.

567 Mookherjee, M., Stixrude, L., Karki, B.B., 2008. Hydrous silicate melt at
568 high pressure. Nature **452**, 983-986.

569 Nevins, D., Spera, F.J., Ghiorso, M.S., 2009. Shear viscosity and diffusion in
570 liquid $MgSiO_3$: Transport properties and implications for terrestrial planet
571 magma oceans. Am. Mineral. **94**, 975-980.

572 Nosé, S., Klein, M.L., 1983. Constant pressure molecular dynamics for molec-
573 ular systems. Mol. Phys. **50**, 1055-1076.

574 Ohtani, E., Kumazawa, M., 1981. Melting of forsterite Mg_2SiO_4 up to 15
575 GPa. Phys. Earth Planet. Inter. **27**, 32-38.

576 Poe, B.T., McMillan, P.F., Rubie, D.C., Chakraborty, S., Yarger, J., Diefen-
577 bacher, J., 1997. Silicon and oxygen self-diffusivities in silicate liquids mea-
578 sured to 15 gigapascals and 2800 Kelvin. Science **276**, 1245-1248.

579 Poe, B.T., Rubie, D.C., 2000. Transport Properties of Silicate Melts at High
580 Pressure, Chapter 6.2 in H. Aoki et al. (eds.), Physics meets Mineralogy,
581 Cambridge University Press, pp.340-353.

582 Presnall, D.C., Walter, M.J., 1993. Melting of Forsterite, Mg_2SiO_4, from 9.7
583 to 16.5 GPa. J. Geophys. Res. **98**, 19777-19783.

584 Reid, J.E., Poe, B.T., Rubie, D.C., Zotov, N., Wiedenbeck, M., 2001. The
585 self-diffusion of silicon and oxygen in diopside ($CaMgSi_2O_6$) liquid up to
586 15 GPa. Chem. Geol. **174**, 77-86.

587 Reid, J.E., Suzuki, A., Funakoshi, K., Terasaki, H., Poe, B.T., Rubie, D.C.,
588 Ohtani, E., 2003. The viscosity of $CaMgSi_2O_6$ liquid at pressures up to 13
589 GPa. Phys. Earth Planet. Inter. **139**, 45-54.

590 Rigden, S.M., Ahrens, T.J., Stolper, E.M., 1989. High-pressure equation of
591 state of molten anorthite and diopside. J. Geophys. Res. **94**, 9508-9522.

592 Righter, K., 2003. Metal-silicate partitioning of soderophile elements and core
593 formation in the early Earth. Annu. Rev. Earth Planet. Sci. **31**, 135-174.

594 Roscoe, R., 1952. The viscosity of suspensions of rigid spheres. British J.
595 Appl. Phys. **3**, 267-269.

596 Rubie, D.C., Melosh, H.J., Reid, J.E., Liebske, C., Righter, K., 2003. Mecha-
597 nisms of metal-silicate equilibration in the terrestrial magma ocean. Earth
598 Planet. Sci. Lett. **205**, 239-255.

599 Rubie, D.C., Frost, D.J., Mann, U., Asahara, Y., Tsuno, K., Nimmo, F.,
600 Kegler, P., Holzheid, A., Palme, H., 2011. Heterogeneous accretion, com-
601 position and core-mantle differentiation of the Earth. Earth Planet. Sci.
602 Lett. **301**, 31-42.

603 Shannon, R.D., Prewitt, C.T., 1969. Effective ionic radii in oxides and fluo-
604 rides. Acta Cryst. B **25**, 925-946.

605 Shimizu, N., Kushiro, I., 1984. Diffusivity of oxygen in jadeite and diopside
606 melts at high pressures. Geochim. Cosmochim. Acta **48**, 1295-1303.

607 Shraiman, B.I., Siggia, E.D., 1990. Heat transport in high-Rayleigh-number
608 convection. Phys. Rev. A **42**, 3650-3653.

609 Solomatov, V. S., 2007. Magma oceans and primordial mantle differentiation,
610 in *Treatise on Geophysics*, edited by G. Schubert, Elsevier, **9**, 91-120.

611 Solomatov, V.S., Stevenson, D.J., 1993. Suspension in convective layers and
612 style of differentiation of a terrestrial magma ocean. J. Geophys. Res. **98**,
613 5375-5390.

614 Solomatov, V.S., Stevenson, D.J., 1993. Kinetics of crystal growth in a ter-
615 restrial magma ocean. J. Geophys. Res. **98**, 5407-5418.

616 Stixrude, L., Karki, B., 2005. Structure and freezing of $MgSiO_3$ liquid in
617 Earth's lower mantle. Science **310**, 297-299.

618 Stixrude, L., de Koker, N.P., Sun, N., Mookherjee, M., Karki, B.B., 2009.
619 Thermodynamics of silicate liquids in the deep Earth. Earth Planet. Sci.
620 Lett. **278**, 226-232.

621 Sun, N., 2008. Magma in Earth's Lower Mantle: First Principle Molecu-
622 lar Dynamics Simulations of Silicate Liquids. Ph.D. Thesis. University of
623 Michigan.

624 Sun, N., Stixrude, L., de Koker, N., Karki, B.B., 2011. First principles molec-
625 ular dynamics simulations of diopsidenext term ($CaMgSi_2O_6$) liquid to high
626 pressure. Geochim. Cosmichim. Acta **75**, 3792-3802.

627 Tangemann, J.A., Phyllips, B.L., Navrotsky, A., Weber, J.K.R., Hixson,
628 A.D., Key, T.A., 2001. Vitreous forsterite (Mg_2SiO_4): Synthesis, structure,
629 and thermochemistry. Geophys. Res. Lett. **28**, 2517-2520.

630 Tonks, W.B., Melosh, H.J., 1993. Magma Ocean Formation Due to Giant
631 Impacts. J. Geophys. Res. **98**, 5319-5333.

Tronnes, R., Frost, D.J., 2002. Peridotite melting and mineral-melt partitioning of major and minor elements at 22-24.5 GPa. Earth Planet. Sci. Lett. **197**, 117-131.

Urbain, G., Bottinga, Y., Richet, P., 1982. Viscosity of liquid silica, silicates and alumino-silicates. Geochim. Cosmochim. Acta **46**, 1061-1072.

Walter, M., Tronnes, R., 2004. Early Earth Differentiation. Frontiers, Earth Planet. Sci. Lett. **225**, 253-269.

Wood, B.J., Walter, M.J., Wade, J., 2006. Accretion of the Earth and segregation of its core. Nature **441**, 825-833.

Yuen, D. A., Hansen, U., Zhao, W., Vincent, A.P., Malevsky, A.V., 1993. Hard Turbulent Thermal Convection and Thermal Evolution of the Mantle. J. Geophys. Res. **98**, 5355-5373.

Zhang, L., Van Orman J.A., Lacks, D.J., 2010. Molecular dynamics investigation of MgO-CaO-SiO_2 liquids: Influence of pressure and composition on density and transport properties. Chem. Geol. **275**, 50-57.

Zhang, J.Z., Herzberg, C., 1994. Melting experiments on anhydrous peridotite KLB-1 from 5.0 to 22.5 GPa. J. Geophys. Res.-Solid Earth **99**, 17729-17742.

	X_0	E_a (kJ/mol)	V_a (cc/mol)
Diffusivity D_O	$(381 \pm 26)\cdot 10^{-9}$ m^2 s^{-1}	125 ± 2	0.710 ± 0.011
Diffusivity D_{Si}	$(331 \pm 21)\cdot 10^{-9}$ m^2 s^{-1}	128 ± 2	0.876 ± 0.009
Diffusivity D_{Mg}	$(635 \pm 26)\cdot 10^{-9}$ m^2 s^{-1}	116 ± 1	1.436 ± 0.007
Viscosity η	$(23.6 \pm 3.2)\cdot 10^{-5}$ Pa s	83 ± 4	1.344 ± 0.021

Table 1: Parameters derived from fitting an Arrhenius relation to self-diffusivity (eq. 3) and viscosity (eq. 4). X_0 refers to D_0 and η_0, respectively.

	0 GPa	
	O^{2-}	SiO_4^{4-}
$\lambda_1\lambda_2\lambda_3$ (Å^3)	23.21	92.84
λ_1 (Å)	0.94	1.72
$(\lambda_2\lambda_3)^{1/2}$ (Å)	4.96	7.35
	32 GPa	
	O^{2-}	SiO_4^{4-}
$\lambda_1\lambda_2\lambda_3$ (Å^3)	15.42	61.71
λ_1 (Å)	1.22	1.93
$(\lambda_2\lambda_3)^{1/2}$ (Å)	3.56	5.64

Table 2: Calculated jump distances λ_1 and $(\lambda_2\lambda_3)^{1/2}$ for the diffusion of O^{2-} and SiO_4^{4-} at 0 GPa and 32 GPa (3000 K).

Property	deep magma ocean (32 GPa)	whole mantle molten
g (m s^{-2})	8	10
r (km)	5100	6370
L (km)	750	2740
ΔT (K)	700	2300
α (K^{-1})	$5 \cdot 10^{-5}$	$2 \cdot 10^{-5}$
c_P (J kg^{-1}K^{-1})	250	250
ρ (g cm^{-3})	2.65	3.0
k (W m^{-1}K^{-1})	1.0	3.0
η (Pa s)	$4 \cdot 10^{-2}$	$6 \cdot 10^{-2}$
Ra	$\sim 10^{28}$	$\sim 10^{29}$
Pr	~ 10	~ 5
q (W)	$\sim 10^{18}$	$\sim 10^{19}$

Table 3: Magma ocean properties based on thermodyamic parameters and viscosity for Mg_2SiO_4 melt and two scenarios of magma ocean dimensions.

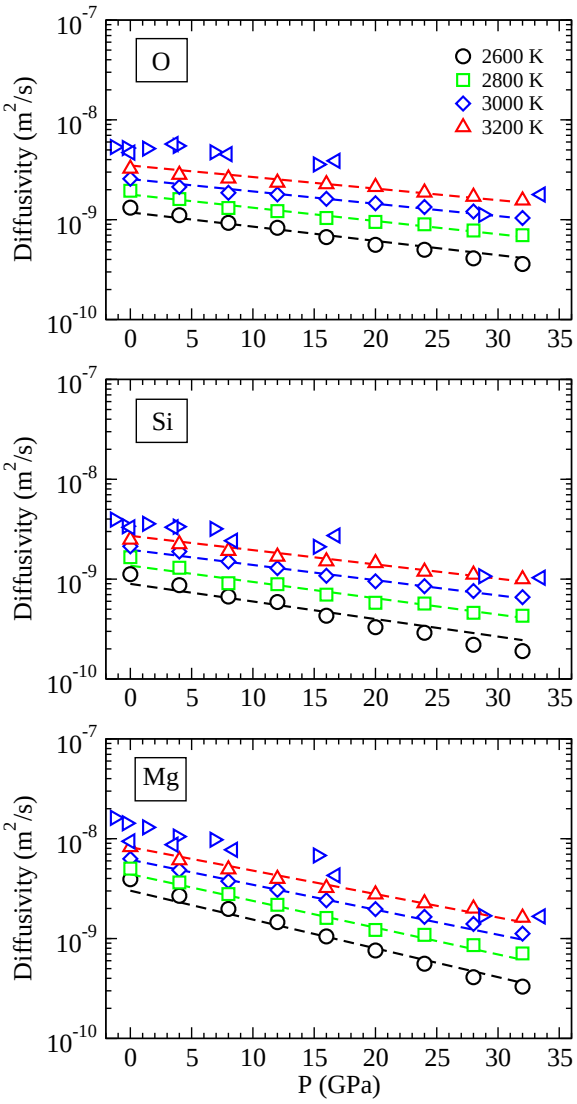

Figure 1: Pressure and temperature dependence of self-diffusivity for O, Si, and Mg in Mg_2SiO_4 melt. Values at different temperatures are shown by symbols and colors. The dashed lines represent the fit to the Arrhenius relation for self-diffusivity (Table 1). Triangles left show self-diffusivity results from *ab-initio* computations at 3000 K (Ghosh and Karki, 2011) and triangles right are from rigid ion simulations at 3000 K (Lacks *et al.*, 2007).

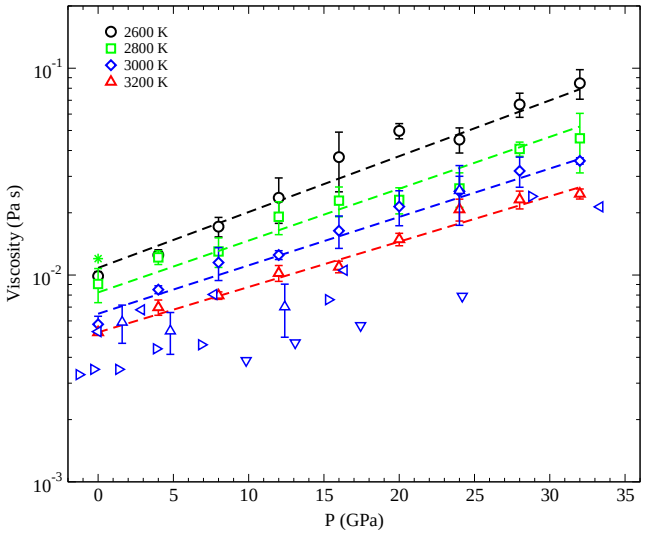

Figure 2: Pressure and temperature dependence of viscosity for Mg_2SiO_4 melt. Values at different temperatures are shown by symbols and colors. The dashed lines represent fits to Arrhenius relation for viscosity (Table 1). The viscosity results at 3000 K (blue symbols) for rigid ion simulations are from Lacks *et al.* (2007) (triangles right) and Martin *et al.* (2009) (triangles down), *ab-initio* simuations from Ghosh and Karki (2011) (triangles left). The star shows ambient pressure viscosity for Mg_2SiO_4 from experiments, extrapolated to 2800 K (Urbain *et al.*, 1982). For comparison η from *ab-initio* simulations on $MgSiO_3$ at 3000 K are included (blue triangles up) (Karki and Stixrude, 2010).

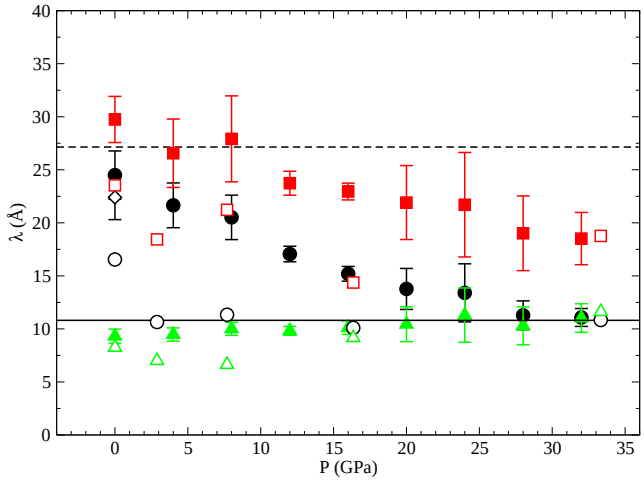

Figure 3: Pressure dependence of diffusion length λ, relating viscosity to self-diffusivity. The calculated λ values using the self-diffusivity of the atomic spieces are shown for oxygen (filled circles), silicon (filled squares) and magnesium (filled triangles up). For comparison (open symbols) the self-diffusivity values for O, Si and Mg at 3000 K from the *ab-initio* simulations are included (Ghosh and Karki, 2011). The open diamond is the result from a rigid ion simulation for O at 0 GPa (Lacks *et al.*, 2007). The lines are the Stokes-Einstein relation with free slip boundary conditions using the ionic radius of Mg^{2+} (0.86 Å, solid line) and the radius of SiO_4^{4-} tetrahedra (2.16 Å, dashed line), respectively.

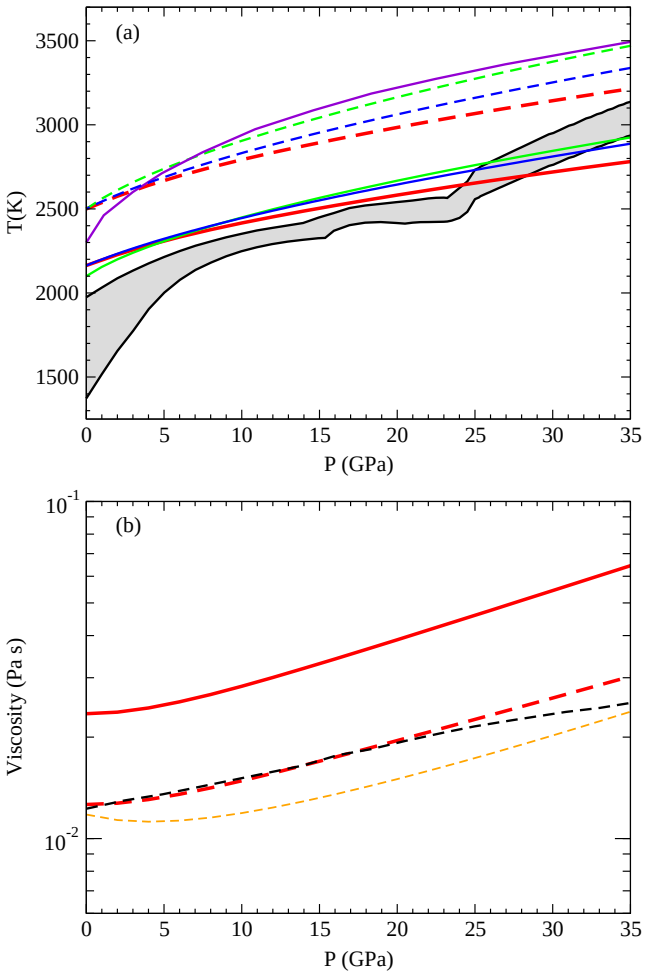

Figure 4: (a) Adiabatic temperature profiles of a forsterite magma ocean with potential temperatures of T_0 = 2163 K (solid red line) and T_0 = 2500 K (dashed red line) based on previously published thermodynamic parameters of Mg_2SiO_4 melt (Adjaoud *et al.*, 2008). Alternative magma ocean adiabats from Stixrude *et al.* (2009) (green) and de Koker and Stixrude (2009) (blue) with the same footing temperatures are shown, as well as the experimentally determined komatiite adiabat (Miller *et al.*, 1991) (purple). The mantle melting interval (grey shaded area) is constrained by experiments to 25 GPa by experiments (Ito *et al.*, 2004; Tronnes and Frost, 2002; Zhang and Herzberg, 1994) and at higher P by simulations of $MgSiO_3$ melting (Stixrude and Karki, 2005). (b) Corresponding viscosity profiles from our simulations (red lines) using the Arrhenius fit (Table 1) for T_0 = 2163 K (solid line) and T_0 = 2500 K (dashed line). For comparison the viscosity profiles from *ab-initio* simulations for Mg_2SiO_4 (golden) (Ghosh and Karki, 2011) and $MgSiO_3$ (black) (Karki and Stixrude, 2010) liquids along our adiabat with T_0= 2500 K are shown.